Journal of the Serbian Society for Computational Mechanics / Vol. 17 / No. 2, 2023 / pp 16-26
(10.24874/jsscm.2023.17.02.02)

NUMERICAL SIMULATIONS OF BLOOD FLOW THROUGH LEFT VENTRICLE USING SPH AND FVM METHODS – A COMPARATIVE STUDY

Marko Topalović[1], Aleksandar Bodić[2*], Miloš S. Pešić[1], Miljan S. Milošević[1,3] and Miroslav M. Živković[2]

[1] University of Kragujevac, Institute for Information Technologies, Kragujevac, Serbia
[2] University of Kragujevac, Faculty of Engineering, Kragujevac, Serbia
e-mail: abodic@uni.kg.ac.rs
[3] Belgrade Metropolitan University, Belgrade, Serbia
**corresponding author*

Abstract

This paper presents a comparative analysis of numerical simulations of blood flow through the left ventricle using SPH (LS-DYNA) and FVM (Ansys Fluent) solvers. Numerical simulations based on SPH and FVM methods can provide a more comprehensive understanding of cardiac blood flow patterns. In Fluent, left ventricle walls were modeled as boundary conditions with zero fluid velocity, while in the LS-DYNA software the walls were modeled with fixed particles. Boundary conditions were also prescribed on the appropriate regions (inlet, outlet, symmetry). In both programmes, inlet and outlet velocities were defined using table functions corresponding to the real cardiac cycle. For generating fluid flow in SPH, injection particles at mitral valve and deactivation planes at aortic semilunar valve were used. Numerical analysis results are given comparatively in both cases at the corresponding times. By comparing the results, it can be concluded that SPH can be efficiently used for the analysis of blood flow through the left ventricle. Although the modeling procedure, as well as the calculation itself, takes much longer to execute using SPH, this method offers possibilities such as studying FSI phenomena or tracking the movement of particles through the fluid domain.

Keywords: SPH, FVM, Left Ventricle, Fluid Flow, Bioengineering.

1. Introduction

Despite significant progress made in the field of medicine, cardiovascular diseases remain the leading cause of death worldwide. Consequently, there has been a notable increase in the number of studies related to heart assessment. The comprehension of cardiac blood flow patterns has various applications, ranging from the examination of hemodynamics to the clinical evaluation of heart performance (Moosavi, et al. 2014). Numerous experimental techniques, including Doppler ultrasound echocardiography (Pedrizzetti, et al. 2014, Mele, et al. 2019) and magnetic resonance imaging (MRI) (Elbaz, et al. 2016, Eriksson, et al. 2011), are commonly used for investigating blood flow patterns. Although these techniques have provided significant results

and as extensive information on blood flow, there is still plenty of room for improvement, especially in terms of enhancing spatial and/or temporal resolution (Xu and Kenjereš 2021).

In addition to experimental techniques, computer simulations such as computational fluid dynamics (CFD) are also used for these purposes. These simulations are usually based on the finite volume method (FVM), finite element method (FEM), and smoothed particle hydrodynamics (SPH). The advantage of these methods is their ability to offer a more comprehensive understanding of blood flow, compared to traditional approaches.

SPH is a mesh-free numerical method (Liu and Liu 2003) based on continuum mechanics, where the considered continuum is subdivided into pseudo-particles known as sub-domains (Vignjević and Campbell 2011). Initially developed for solving astrophysical problems (Gingold and Monaghan 1997, Lucy 1977), SPH has been extended to CFD (Monaghan and Pongracic 1985) and solid mechanics (Libersky, et al. 1993). It is based on the application of the Lagrangian material framework for tracking the movement of a specific domain section, regardless of its state or composition (Liu and Liu 2003). On the other hand, the FVM, which also relies on continuum mechanics, is based on the application of Eulerian spatial formulation to observe a fixed volume through which the fluid flows (Ansys Inc. - Theory Guide 2013). Figure 1 illustrates the difference between these two approaches on the example of the finite element method (Bathe 2006), which can use both approaches.

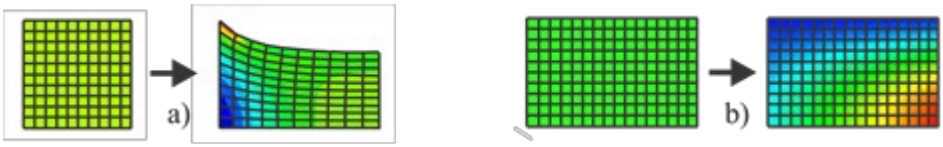

Fig. 1. Difference between a) Lagrangian and b) Eulerian numerical formulation.

This paper presents a comparison of numerical simulations of blood flow through the left ventricle using commercially available smoothed particle hydrodynamics (SPH) and finite volume method (FVM) solvers (LS-DYNA and Ansys Fluent). Modeling of cardiovascular systems using the SPH method requires the definition of comprehensive boundary conditions (Vacondio, et al. 2021), high computational requirements, and time to obtain accurate results. The main objective of this paper is to address these challenges and facilitate the application of the SPH method in bioengineering numerical simulations (Kojić, et al. 2008).

Ansys Fluent was used to model blood flow through the left ventricle using FVM. The results obtained using the FVM method were used as a verification of the results obtained using the SPH method.

The rest of the paper is organized as follows: Chapter 2 provides a brief retrospective of the SPH kernel and particle approximation, along with the procedure for modeling the left ventricle using the SPH method within the LS-DYNA software. In chapter 3, governing equations of fluid dynamics and the procedure for left ventricle numerical analysis using the FVM in the Ansys Fluent software are presented. Chapter 4 compares the results obtained from both methods. Finally, the conclusion summarizes the outcomes presented in the paper and outlines potential areas for future research.

2. Numerical analysis of blood flow through left ventricle

Numerical analyses of blood flow through the left ventricle were performed using SPH and FVM, as mentioned in the previous chapter. LS-DYNA software was used for numerical analysis of the left ventricle using SPH, while Ansys Fluent was employed for the numerical analysis of the left ventricle using FVM. The geometry of the left ventricle (Fig. 2), considered in both analyses, was created using CAD Solid and Field software (Milošević 2022). In this study, a parameterized model of the heart was considered, which, although simplified, incorporated geometric parameters obtained from the patient data (Tomasević S., et al. 2023).

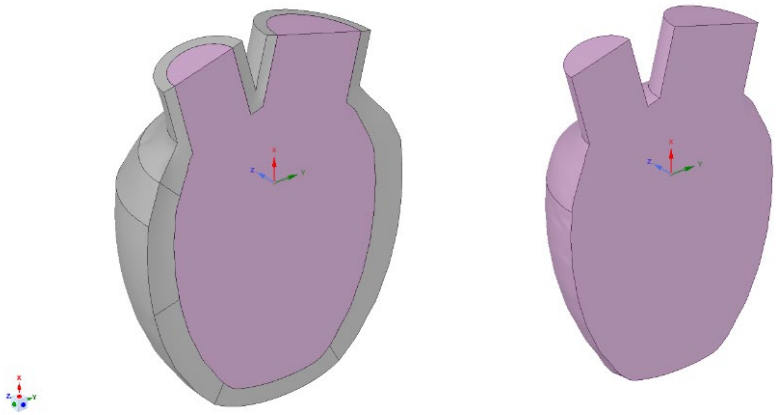

Fig. 2. Geometry of parametric left ventricle model.

As can be seen from Fig. 2, this model consists of the left ventricle wall and a domain within the wall through which the blood flows. Within the numerical simulation using FVM in Fluent, only the geometry of the fluid domain was used. The wall itself was not modeled, but the wall boundary condition was defined on the fluid domain surfaces that coincide with the inner wall surface. On the other hand, within the numerical simulation using SPH in the LS-DYNA, only the wall geometry was used. The LV wall was modeled using fixed solid SPH particles. The fluid domain was filled with initial particles, and after that, new particles with prescribed velocities were injected into the fluid domain.

Both analyses focused on investigating the blood-flow pattern through the left ventricle (CFD analysis). Therefore, it should be noted that the fluid-solid interaction was not considered in this paper.

Material parameters of blood used in both programmes are given in Table 1.

Material Parameter	Value
Density ρ [kg/m^3]	1060
Viscosity μ [Pa·s]	0.001

Table 1. Material parameters of blood.

In both programmes, velocities corresponding to the realistic cardiac cycle were defined at the inlet and outlet (Tomasević S., et al. 2023). These velocities at the inlet (mitral valve) and the outlet (aortic valve) cross-sections were defined by the functions shown in Fig. 3.

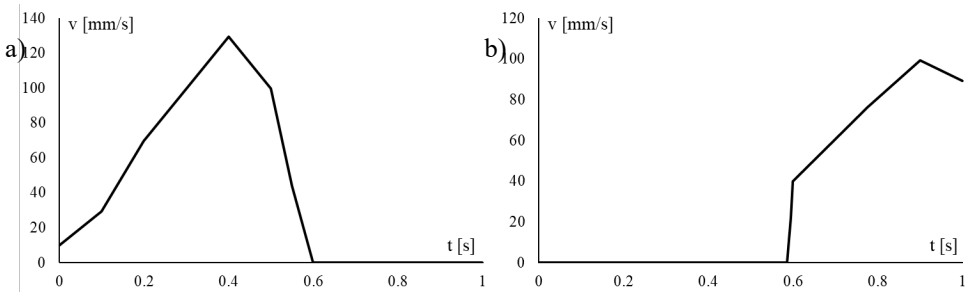

Fig. 3. Functions used to define a) inlet and b) outlet velocities of the model.

In the first approximately 0.5 s, mitral valve is opened and the blood flows into the left ventricle from the atrium part (Fig. 3a). After that, due to the ventricle contraction, blood is forced out through the aortic valve. The velocity of the blood at the outlet can be defined by the function shown in Fig. 3b.

3 SPH numerical analysis

3.1 Theoretical Basis of SPH method

In the SPH method, continuous matter is defined by applying the kernel and particle approximation (Liu and Liu 2003) to the laws of conservation of mass and momentum, given by the partial differential equations. These equations can be transformed into integral equations with interpolation functions which estimate field variables at specific points. The exact value of the function $f(\mathbf{x})$ in integral form is given with the expression:

$$f(\mathbf{x}) = \int_{\Omega} f(\mathbf{x}')\delta(\mathbf{x}-\mathbf{x}')d\mathbf{x}' \tag{1}$$

where $f(\mathbf{x})$ is a function of the position vector $\mathbf{x}$ of the observed pseudo-particle, $\mathbf{x}'$ represents the position vector of the material point which belongs to the domain of influence Ω, and $\delta(\mathbf{x}\text{-}\mathbf{x}')$ is Dirac's measure.

Due to its nature, the Dirac measure is not suitable for use in computational applications, and because of that is replaced with bell-shaped kernel function $W(|\mathbf{x}\text{-}\mathbf{x}'|, h)$, where h represents smoothing length (bell base radius) (Fig. 4).

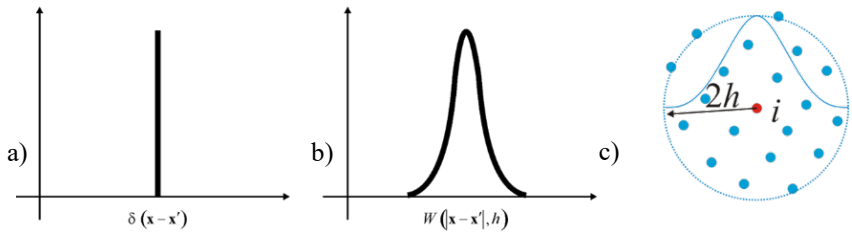

Fig. 4. a) Dirac's measure; b) bell-shaped function; c) smoothing length.

In this way, the kernel approximation of the function $f(\mathbf{x})$ is obtained (Liu and Liu 2003):

$$\left\langle f(\mathbf{x})\right\rangle = \int_{\Omega} f(\mathbf{x}')W\left(\left|\mathbf{x}-\mathbf{x}'\right|,h\right)d\mathbf{x}' \tag{2}$$

The numerical implementation of integral form expressed with equation (2) is not possible because the analyzed continuous matter is divided into finite number of particles, where each particle has its own mass and occupies individual space. Therefore, equation (2) is transformed into a discrete form, which can be defined as a sum over all particles within the support domain. The infinitesimal volume d$\mathbf{x}'$ can be replaced with finite volume of particle $\Delta V_\beta = m_\beta/\rho_\beta$, where m_β and ρ_β are particle mass and density. Summing over all particles within support domain gives us a particle approximation of function $f(\mathbf{x})$ for the observed particle α (Liu and Liu 2003):

$$\left\langle f(\mathbf{x}_\alpha)\right\rangle \cong \sum_{\beta=1}^{NNP} f(\mathbf{x}_\beta)W\left(\left|\mathbf{x}_\alpha-\mathbf{x}_\beta\right|,h\right)dV_\beta = \sum_{\beta=1}^{NNP}\frac{m_\beta}{\rho_\beta}f(\mathbf{x}_\beta)W\left(\left|\mathbf{x}_\alpha-\mathbf{x}_\beta\right|,h\right) \tag{3}$$

where NNP is the number of the nearest neighbouring particles.

Equation (3) incorporates kernel and particle approximations. Using this equation, the laws of conservation of mass and momentum are implemented in SPH solvers. These solvers use an explicit integration scheme to calculate velocities, accelerations, displacements, etc. The total stress tensor σ_{ij} in a viscous fluid consists of hydrostatic pressure p and viscous stress ${}^{vics}\tau_{ij}$:

$$\sigma_{ij} = -p\delta_{ij} + {}^{visc}\tau_{ij} \tag{4}$$

where viscous stress can be expressed with equation:

$${}^{visc}\tau_{ij} = \mu\left(\partial_i v_j + \partial_j v_i - \frac{2}{3}\partial_k v_k \delta_{ij}\right) = \mu\varepsilon_{ij} \tag{5}$$

where μ represents the coefficient of dynamic viscosity and ε_{ij} represents the strain rate tensor (Liu and Liu 2003):

$$\varepsilon_{ij}^{\alpha} = \sum_{\beta=1}^{NNP}\frac{m_\beta}{\rho_\beta}v_j^{\beta\alpha}\frac{\partial W^{\alpha\beta}}{\partial x_i^{\alpha}} + \sum_{\beta=1}^{NNP}\frac{m_\beta}{\rho_\beta}v_i^{\beta\alpha}\frac{\partial W^{\alpha\beta}}{\partial x_j^{\alpha}} - \left(\frac{2}{3}\sum_{\beta=1}^{NNP}\frac{m_\beta}{\rho_\beta}\mathbf{v}^{\beta\alpha}\cdot\nabla_\alpha W^{\alpha\beta}\right)\delta_{ij} \tag{6}$$

Hydrostatic pressure p can be calculated using the Murnaghan equation of state (Liu and Liu 2003):

$$p = k_0\left[\left(\frac{\rho}{\rho_0}\right)^{\gamma} - 1\right] \tag{7}$$

where ρ_0 is the fluid density at rest, while k_0 and γ are material parameters.

3.2 Left ventricle modelling in LS-DYNA

For the numerical simulation of blood flow through left ventricle using the SPH method, the LS-DYNA software (LS-DYNA Theory Manual 2022) was employed. The primary research and development focus of this commercial software is not on fluid flow analysis using SPH particles, especially in the field of bioengineering. Several academic or open-source SPH solvers can be found in numerous published papers or examples, offering various approaches for generating and removing SPH particles. The LS-DYNA manual provides detailed explanations of keywords BOX, BOX_LOCAL, BOUNDARY_SPH_FLOW, SPH_INJECTION, PRESCRIBED_MOTION_SET_BOX, CONTROL_SPH (BOXID), and

SET_NODE_LIST_GENERATE. These keywords enable the activation or deactivation of SPH particles and are used to create the variable fluid flow defined by functions shown in Fig. 3.

In older versions of the LS-DYNA software (before R12 from 2020), there was no way to generate new SPH particles with variable velocities. New particles could only be generated at a constant velocity, posing significant challenges for this type of analysis. The only available solution was to use BOUNDARY_SPH_FLOW keyword with a long streak of SPH particles that are activated when they reach activation plane, as can be seen in Fig. 5.

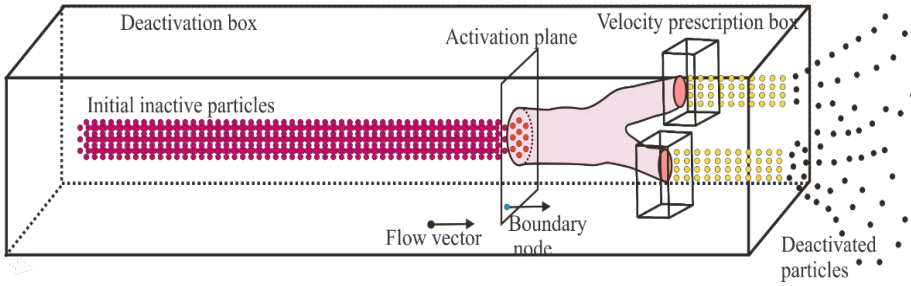

Fig. 5. Obsolete generation of fluid flow using BOUNDARY_SPH_FLOW keyword.

In the latest version of LS-DYNA, to prescribe variable velocity, a negative injection speed scale factor needs to be set for the SPH_INJECTION keyword. This assigns the value from the DEFINE_CURVE keyword to the scale factor instead of a constant value for the velocity. The problem with this approach is that new SPH particles can collide with existing ones and bounce away or cause an explosion. To avoid this, the PRESCRIBE_MOTION_SET_BOX keyword is utilized, which generates a box in front of the injected particles, and within which the DEFINE_CURVE keyword can be used to define particle velocity functions, i.e., functions from Fig. 3. Similarly, particle velocities at the aortic semilunar valve (outlet of the model) can be defined. Since these keywords do not define motion of all SPH particles, but only particles specified in the NODE_LIST keyword, PRESCRIBED_MOTION_SET_BOX keyword is used twice at the outlet: once with NODE_LIST for preexisting particles and the second time with NODE_LIST_GENERATE for the new, injected particles. Schematic representation of the Left Ventricle SPH model is illustrated in Fig. 6.

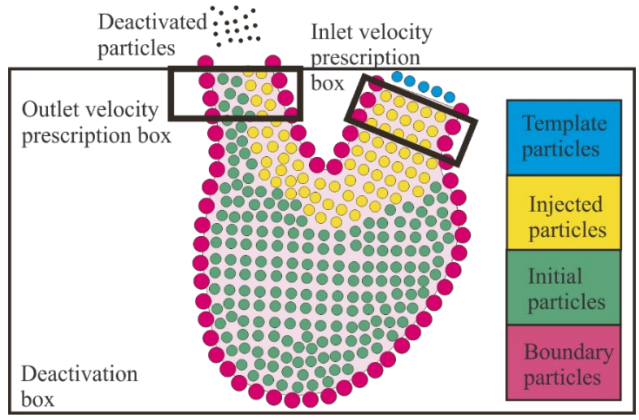

Fig. 6. Schematic representation of Left Ventricle SPH model with all used keywords.

The geometry of the LV wall was used for generating finite elements, which were subsequently converted into SPH solid particles, marked in red in Fig. 6. Before the beginning of the simulation, the initially empty fluid domain is filled with particles marked in green. Once the fluid domain was filled with initial particles, prescribed with constant velocity, the simulation started by assigning the velocity to template particles (blue color) according to Fig. 3a. Template particles were then duplicated into newly generated particles (yellow) and moved toward the inlet velocity prescription box. Upon reaching the inlet velocity prescription box, the velocity of the yellow particles was prescribed using same function as for template particles. It was crucial to prescribe velocity to both template and existing particles within the box to prevent newly generated particles from bouncing off existing ones and returning back. At the LV outlet, velocity was prescribed according to Fig. 3b to all particles that reach the outlet velocity prescription box. Finally, all particles that reached outside the deactivation box were deleted.

4 FVM numerical analysis

Blood flow through the left ventricle is considered as laminar flow of incompressible fluid and can be defined by Navier-Stokes equations and continuity equation (Kojić, et al. 2008):

$$-\mu\nabla^2 v_l+\rho\left(v_l\cdot\nabla\right)v_l+\nabla p_l=0 \tag{8}$$

$$\nabla v_l=0 \tag{9}$$

where v_l is fluid velocity, p_l is the pressure, μ represents coefficient of dynamic viscosity and ρ is fluid density.

A numerical analysis of the left ventricle using FVM was performed in Ansys Fluent software. Based on the geometry of the left ventricle from Fig. 2, a finite volume mesh was created within Fluent Meshing. The mesh was generated using tetrahedral finite volume cells. A mesh independence study was performed, where a model was created with different cell size in order to define the optimal cell size. The cell size was set to 2 mm, and the entire model consisted of 62208 cells and 11972 nodes. The quality of the mesh was checked using Fluent Meshing, and maximum cell skewness was 0.84. The finite volume mesh of the left ventricle is shown in Fig. 7.

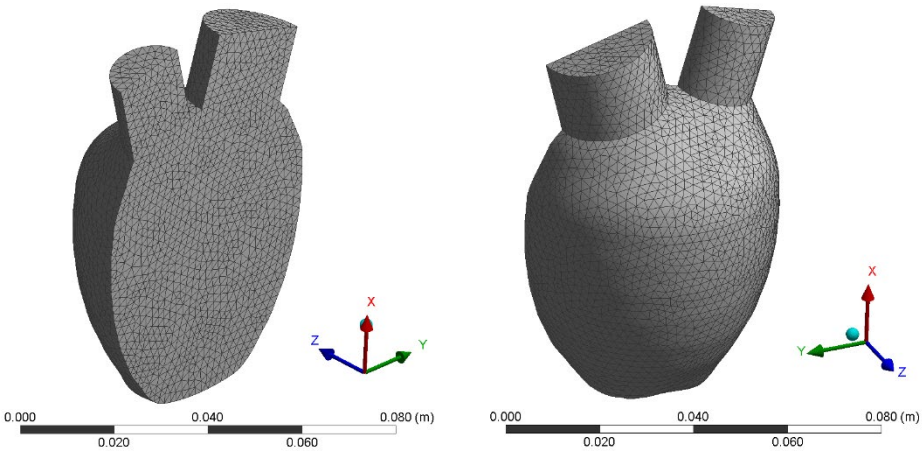

Fig. 7. Finite volume mesh of left ventricle.

On the left ventricle model, specific regions (named selections) representing the inlet, outlet, symmetry and wall were defined. Based on these regions, boundary conditions were set on the model (Fig. 8). The inlet and outlet prescribed velocities were set to correspond to the functions in Fig. 3. Two User Defined Functions (UDF) were created for these purposes. Since the velocity at the outlet region could not be prescribed in the version of Fluent used for this research, the model consisted of "two inlet regions". Therefore, at the inlet region from the atrium part, the velocity was set using a UDF script to correspond to the function shown in Fig. 3a. On the other hand, at the "inlet region of the aortic valve" (outlet of the model), the velocity was set using a UDF script so that the function shown in Fig. 3b is reversed. In this way, the outflow of blood from the left ventricle through the aortic valve due to the contraction of the heart muscle walls was simulated.

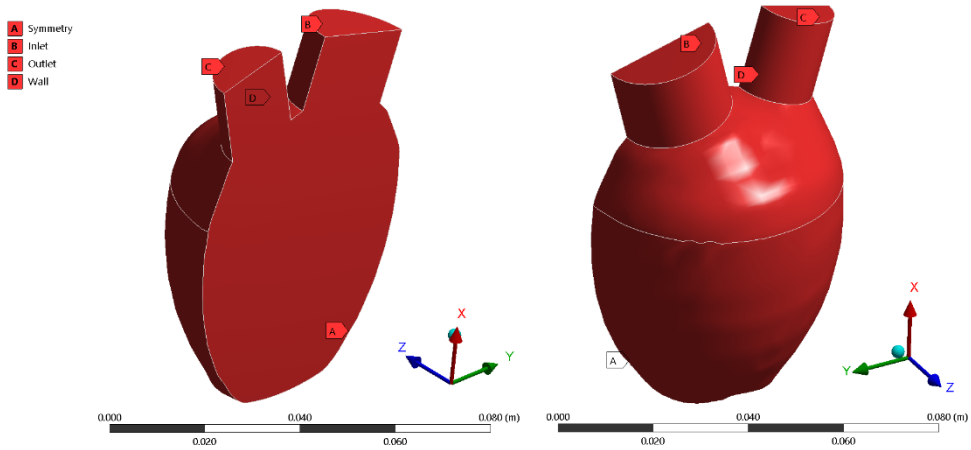

Fig. 8. Named selections set on the left ventricle model.

Time step independence study was also performed before final analysis in order to reach the optimal number of steps and step size. The adopted value for time step size was 0.002 s. Therefore, a transient analysis was performed in 500 time steps.

3. Results and Discussion

As can be seen in Fig. 3, the inlet velocity reaches its maximum value in 0.4 s. Therefore, Fig. 9 shows a comparison of the velocity field at that particular time obtained in both programmes. The outlet velocity reaches maximum value at 0.9 s, but at that time fluid velocities within ventricle volume are negligible. For that reason, a comparison of velocity fields obtained in both programmes is given at a more appropriate time of 0.8 s (Fig. 10).

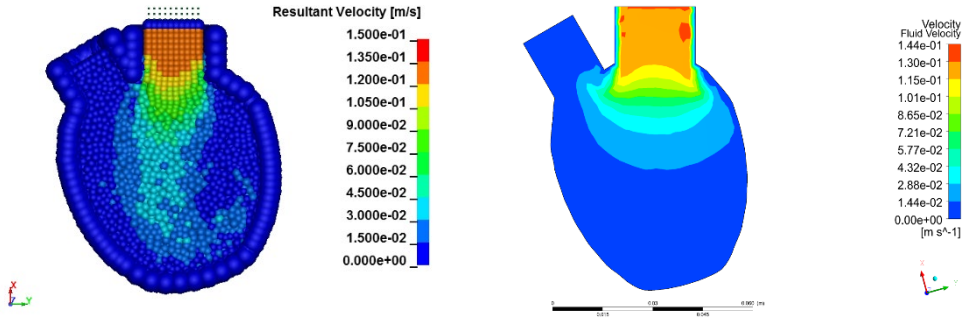

Fig. 9. Velocity field at 0.4 s in a) LS-DYNA and b) Fluent.

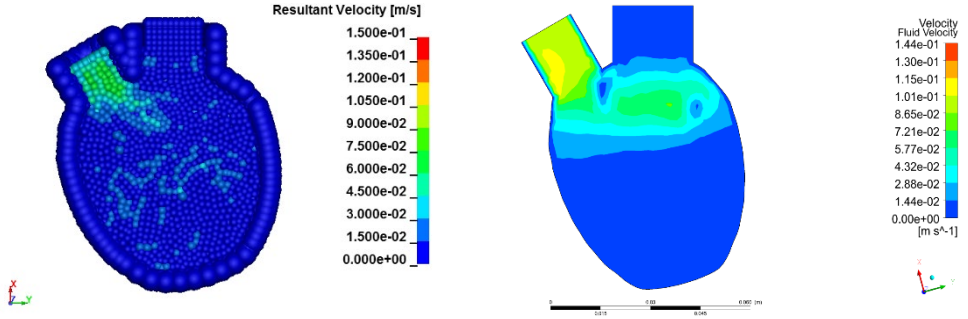

Fig. 10. Velocity field at 0.8 s in a) LS-DYNA and b) Fluent.

Figure 11 shows a comparison of the time dependence of maximum velocity value in in Fluent and LS-DYNA.

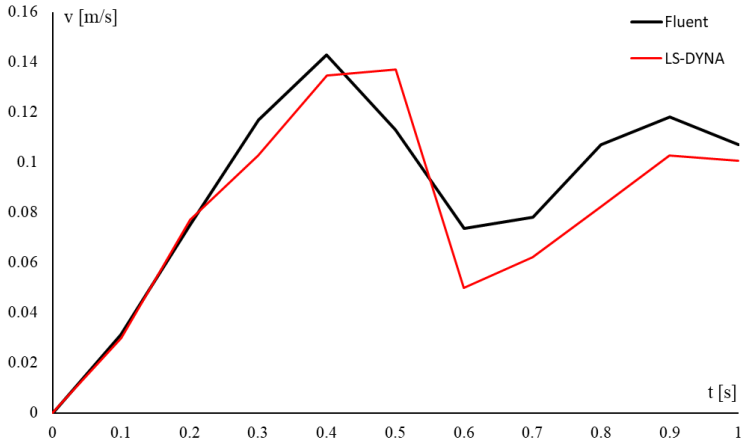

Fig. 11. Comparison of the time dependence of maximum velocity value in Fluent and LS-DYNA.

Based on the previous figures, it is evident that both the SPH and FVM solvers give similar velocity fields. However, slight differences in the results can be noticed after 0.6 seconds, when the blood begins to flow through the aortic valve. These deviations can be explained by the nature of the SPH method, i.e., oscillations between SPH particles due to a large step. The value of the maximum velocity at each step corresponds to the prescribed velocities at the inlet and outlet of the model with minor deviations in the form of a slight velocity increase caused by the geometry of the model. Additionally, it is important to point out that the SPH analysis took 25 hours to complete, whereas the FVM method only required approximately 30 minutes on an AMD Ryzen 7 5800X with 128 GB DDR4. While the FVM method is undoubtedly the preferable choice for pure CFD simulations, the SPH approach offers flexibility, scalability, and a unified foundation for further research when dealing with multiphysics and multiscale calculations.

4. Conclusions

The main fields of application of the SPH method lies in marine and aeronautical engineering for numerical analyses involving fluid-structure interaction between vessels and surrounding water, as well as predicting bird strikes or crash-landing. However, these applications typically involve static fluid and high-speed impacts. This paper focuses on utilizing SPH for bioengineering analysis, particularly in modeling continuous variable fluid flow. The LS-DYNA software was employed for modelling blood flow through the left ventricle using the SPH method, while the same problem was modeled using FVM in Ansys Fluent for verification purposes.

By comparing the results obtained using both methods, it can be concluded that the LS-DYNA software gives similar results to those obtained in Ansys Fluent. Nevertheless, it is important to note that prescribing boundary conditions in LS-DYNA is more challenging than in Fluent. To achieve realistic blood flow, a combination of keywords in the LS-DYNA input file was utilized, and inlet and outlet velocities were prescribed by defining appropriate boxes. Although the calculation time in SPH software is significantly longer, this method has a great potential for conducting more sophisticated fluid-structure interaction analyses within the Lagrangian material framework, which will be the primary focus of our future research.

Acknowledgements: The authors acknowledge support of the Ministry of Science, Technological Development and Innovation, Republic of Serbia, Agreement No. 451-03-47/2023-01/200378 and Grant TR32036.

References

Ansys Inc. (2013) Theory Guide.

Bathe, K. (2006) Finite element Procedures. Prentice Hall: Pearson Education, Inc., USA.

Elbaz, M.S.M, R.J van der Geest, E.E Calkoen, A de Roos, B.P.F Lelieveldt, A.A.W Roest, and J.J.M Westenberg (2016), Assessment of viscous energy loss and the association with three-dimensional vortex ring formation in left ventricular inflow: In vivo evaluation using four-dimensional flow MRI, Magnetic Resonance in Medicine 77 (2), 794-805.

Eriksson, J, P Dyverfeldt, J Engvall, A.F Bolger, T Ebbers, and C.J Carlhäll (2011), Quantification of presystolic blood flow organization and energetics in the human left ventricle, American Journal of Physiology-Heart and Circulatory Physiology, 300 (6), H2135-H2141.

Gingold, R.A, and J.J Monaghan (1997), Smoothed particle hydrodynamics: theory and application to non-spherical stars, Monthly Notices Royal Astronomy Society, 181, 375-389.

Kojić, M, N Filipović, B Stojanović, and N Kojić (2009), Computer Modeling in Bioengineering: Theoretical Background, Examples and Software, John Wiley & Sons, USA.

Libersky, L.D, A.G Petschek, T.C Carney, J.R Hipp, and F.A Allahdadi (1993), High Strain Lagrangian Hydrodynamics: A Three-Dimensional SPH Code for Dynamic Material Response, Journal of Computational Physics, 109, 67-75.

Liu, G, and M Liu. (2003), Smoothed Particle Hydrodynamics, World Scientific Publishing, Singapore.

Livemore Software Technology Corporation (2022), LS-DYNA Theory Manual.

Lucy, L.B. (1977), A numerical approach to the testing of fusion process, Astronomical Journal, 88, 1013-1024.

Mele, D, V Smarazzo, G Pedrizzetti, F Capasso, M Pepe, S Severino, G.A Luisi, M Maglione, and R Ferrari (2019), Intracardiac Flow Analysis: Techniques and Potential Clinical Applications, J Am Soc Echocardiogr, 32 (3), 319-332.

Milošević, M. (2022), CAD Solid and Field, https://github.com/miljanmilos/CAD-Solid-Field

Monaghan, J.J, and H Pongracic (1985), Artificial viscosity for particle methods, Applied Numerical Mathematics, 109, 67-75.

Moosavi, MH, N Fatouraee, H Katoozian, A Pashaei, O Camara, and Frangi AF (2014), Numerical simulation of blood flow in the left ventricle and aortic sinus using magnetic resonance imaging and computational fluid dynamics, Comput Methods Biomech Biomed Engin, 17 (7), 740-749.

Pedrizzetti, G, G La Canna, O Alfieri, and T Giovanni (2014), The vortex-an early predictor of cardiovascular outcome?, Nat Rev Cardiol, 11 (9), 545-553.

Tomasević S., Milosević, M, B Milicević, V Simić, M Prodanović, S Mijailovich, and N Filipović (2023), Computational Modeling on Drugs Effects for Left Ventricle in Cardiomyopathy Disease, Pharmaceutics, 15 (3), ar.no. 793.

Vacondio, R, C Altomare, M De Leffe, X Hu, D Le Touzé, S Lind, J-C Marongiu, S Marrone, B.D Rogers, and A Souto-Iglesias (2021), Grand challenges for Smoothed Particle Hydrodynamics numerical schemes, Computational Particle Mechanics, 8, 575-588.

Vignjević, R, and J Campbell (2011), Brief review of development of the smooth particle hydrodynamics (SPH) method, Proc. IConSSM 2011 - The 3rd International Congress of Serbian Society of Mechanics. Vlasina lake, Serbia.

Xu, F, and S Kenjereš (2021), Numerical simulations of flow patterns in the human left ventricle model with a novel dynamic mesh morphing approach based on radial basis function, Computers in Biology and Medicine, 130, 104184.